EUMETSAT

The Conversion from Effective Radiances to Equivalent Brightness Temperatures

Doc.No. : EUM/MET/TEN/11/0569
Issue : v1
Date : 5 October 2012
WBS :

EUMETSAT
Eumetsat-Allee 1, D-64295 Darmstadt, Germany
Tel: +49 6151 807-7
Fax: +49 6151 807 555
http://www.eumetsat.int

EUMETSAT

Document Signature Table

	Name	*Function*	*Signature*	*Date*
Prepared by	Stephen Tjemkes	Meteorological Scientist		
Reviewed by	Rolf Stuhlmann	MTG Programme Scientist		
Reviewed by	Tim Hewison	Meteorological Scientist		
Reviewed by	Johannes Müller	Instrument Data Processing Engineer		
Approved	Volker Gärtner	H/USD		
Release authorised by	Sergio Rota	H/GEO		

Distribution List

Name	*No. of Copies*
WEB DISTRIBUTION	1

Document Change Record

Issue / Revision	*Date*	*DCN. No.*	*Changed Pages / Paragraphs*
v1	5 October 2012		New

Contents

1 Introduction **1**

2 Simple relation **2**

3 Coefficients for Meteosat 8 (MSG-FM-1) and 9 (MSG-FM-2) **3**

4 Coefficients for MSG-FM-3 and -4. **4**

5 Summary **5**

6 Reference Documents **6**

7 Tables **7**
7.1 General 7
7.2 Parameter tables 8
7.2.1 Table for Meteosat-8 (MSG FM-1) 8
7.2.2 Table for Meteosat-9 (MSG FM-2) 9
7.2.3 Table for MSG FM-3 9
7.2.4 Table for MSG FM-4 10

8 Figures **11**

List of Tables

7.1 *Values for constants at time of writing [RD.3].* 7

7.2 *Values for the regression parameters ν_c, α and β of the three parameter model evaluated using the non-linear regression analysis. The input LUT of radiances and brightness temperatures was calculated for brightness temperatures between 150 and 350 K with steps of 0.1 K. The values are valid for SEVIRI on Meteosat 8 (MSG Flight Model 1).* 8

7.3 *Values for the regression parameters ν_c, α and β of the three parameter model evaluated using the non-linear regression analysis. The input LUT of radiances and brightness temperatures was calculated for brightness temperatures between 150 and 350 K with steps of 0.1 K. The values are valid for SEVIRI on Meteosat 9 (MSG Flight Model 2).* 9

7.4 *Values for the regression parameters ν_c, α and β of the three parameter model evaluated using the kapteyn non-linear regression module (http://www.astro.rug.nl/software/kapteyn/inde for the different channels on MSG flight model 3. The input LUT of radiances and brightness temperatures were taken from the IMPF radiance and brightness temperatures.* 9

7.5 *Values for the regression parameters ν_c, α and β of the three parameter model evaluated using the kapteyn non-linear regression module ((http://www.astro.rug.nl/software/kapteyn/ina for the different channels on MSG flight model 4. The input LUT of radiances and brightness temperatures were taken from the IMPF radiance and brightness temperatures.* 10

List of Figures

8.1 Result of the non-linear regression for ir 39 on Meteosat 8 (MSG-FM-1). . . . 11
8.2 Result of the non-linear regression for wv 62 on Meteosat 8 (MSG-FM-1). . . . 12
8.3 Result of the non-linear regression for wv 73 on Meteosat 8 (MSG-FM-1). . . . 13
8.4 Result of the non-linear regression for ir 87 on Meteosat 8 (MSG-FM-1). . . . 14
8.5 Result of the non-linear regression for ir 97 on Meteosat 8 (MSG-FM-1). . . . 15
8.6 Result of the non-linear regression for ir 108 on Meteosat 8 (MSG-FM-1). . . . 16
8.7 Result of the non-linear regression for ir 120 on Meteosat 8 (MSG-FM-1). . . . 17
8.8 Result of the non-linear regression for ir 134 on Meteosat 8 (MSG-FM-1). . . . 18
8.9 Result of the non-linear regression for ir 39 on Meteosat 9 (MSG-FM-2). . . . 19
8.10 Result of the non-linear regression for wv 62 on Meteosat 9 (MSG-FM-2). . . . 20
8.11 Result of the non-linear regression for wv 73 on Meteosat 9 (MSG-FM-2). . . . 21
8.12 Result of the non-linear regression for ir 87 on Meteosat 9 (MSG-FM-2). . . . 22
8.13 Result of the non-linear regression for ir 97 on Meteosat 9 (MSG-FM-2). . . . 23
8.14 Result of the non-linear regression for ir 108 on Meteosat 9 (MSG-FM-2). . . . 24
8.15 Result of the non-linear regression for ir 120 on Meteosat 9 (MSG-FM-2). . . . 25
8.16 Result of the non-linear regression for ir 134 on Meteosat 9 (MSG-FM-2). . . . 26
8.17 Result of the non-linear regression for ir 39 on MSG FM3. 27
8.18 Result of the non-linear regression for wv 62 on MSG FM3. 28
8.19 Result of the non-linear regression for wv 73 on MSG FM3. 29
8.20 Result of the non-linear regression for ir 87 on MSG FM3. 30
8.21 Result of the non-linear regression for ir 97 on MSG FM3. 31
8.22 Result of the non-linear regression for ir 108 on MSG FM3. 32
8.23 Result of the non-linear regression for ir 120 on MSG FM3. 33
8.24 Result of the non-linear regression for ir 134 on MSG FM3. 34
8.25 Result of the non-linear regression for ir 39 on MSG FM4. 35
8.26 Result of the non-linear regression for wv 62 on MSG FM4. 36
8.27 Result of the non-linear regression for wv 73 on MSG FM4. 37
8.28 Result of the non-linear regression for ir 87 on MSG FM4. 38
8.29 Result of the non-linear regression for ir 97 on MSG FM4. 39
8.30 Result of the non-linear regression for ir 108 on MSG FM4. 40
8.31 Result of the non-linear regression for ir 120 on MSG FM4. 41
8.32 Result of the non-linear regression for ir 134 on MSG FM4. 42

Abstract

This paper documents the relation between effective radiance and equivalent brightness temperature for the MSG-MPEF. It lists the rationale, method and results for a simple analytical expression to convert the observed effective radiances in $mWm^{-2}sr^{-1}\left(cm^{-1}\right)^{-1}$ to equivalent brightness temperatures in units kelvin.

Chapter 1

Introduction

A satellite instrument measures the upwelling radiation at the top of the atmosphere. Let $L_\nu(p_t, \mu)$ represents the spectral variation of the upwelling radiance at the top of the atmosphere (at pressure p_t) propagating towards the satellite sensor, r_ν represent the spectral response function, ν wavenumber and $\mu = \cos\theta$, with θ is the angle between zenith and viewing direction, then the observed effective radiance $\bar{\mathcal{L}}$is given by:

$$\bar{\mathcal{L}} = \int_{\Delta\nu} r_\nu L_\nu(p_t, \mu) d\nu / \int r_\nu d\nu. \tag{1.1}$$

These observations are expressed in $mWm^{-2}sr^{-1}\left(cm^{-1}\right)^{-1}$. To facilitate an easy interpretation of these observations, these units are converted into equivalent black body temperatures (in kelvin-units) or alternatively known as equivalent brightness temperatures. The brightness temperature is defined as the temperature of a black body which emits the same amount of radiation as observed. Thus the brightness temperature (T_b) follows from

$$\bar{\mathcal{L}} = \int_{\Delta\nu} r_\nu B\left(\nu, T_b\right) d\nu / \int r_\nu d\nu. \tag{1.2}$$

with B the Planck-function. Inversion of Eq. 1.2 is not possible because of the variation of the Planck and the spectral response function (r_ν) with wavenumber.

It is possible to generate a pre-calculated lookup table (LUT) which contains the calculated effective radiance of a black body at a given temperature as observed by the particular instrument using Eq. 1.2. The brightness temperature of an actual observation is found from interpolation in this LUT. This is the method currently adopted by the IMage Processing Facility (IMPF) within the Meteosat Second Generation Ground Segment (MSG-GS) as documented in [RD.1].

Chapter 2

Simple relation

For several applications the search in a pre-calculated LUT is too time consuming and for these a simple relation between observed effective radiance and the corresponding brightness temperature is preferred over the interpolation in a pre-calculated LUT. A simple relation can be derived assuming that the Planck-function is independent of wavenumber over the particular interval:

$$\begin{aligned}\bar{\mathcal{L}} = & \int_{\Delta\nu} r_\nu B\left(\nu, T_b\right) d\nu \Big/ \int_{\Delta\nu} r_\nu d\nu. \\ \approx & \bar{B}\left(T_b\right)\end{aligned} \tag{2.1}$$

where $\bar{B}$ represents a mean value over the interval . Upon substitution in the Planck-function, the simple relation reads:

$$\bar{\mathcal{L}} \approx 2hc^2\nu_c^3 / \left(\exp\left(hc\nu_c/kT_b\right) - 1\right), \tag{2.2}$$

where ν_c represents a representative wavenumber, h the Planck constant, c speed of light and k the Boltzmann constant. Equation 2.2 is a single parameter function. The single parameter (ν_c) can be found from a non-linear regression of the pre-calculated LUT mentioned above. An alternative relation can be found from a generalization of Eq. 2.2:

$$\bar{\mathcal{L}} \approx \gamma / \left(\exp\left(\delta/T_b\right) - 1\right), \tag{2.3}$$

with γ and δ two parameters which can be found from a non-linear regression of the pre-calculated LUT mentioned above. More often a three parameter function is fitted to the LUT:

$$\bar{\mathcal{L}} \approx 2hc^2\nu_c^3 / \left(\exp\left(hc\nu_c/k\left[\alpha T_b + \beta\right]\right) - 1\right), \tag{2.4}$$

with ν_c, α and β three parameters which can be found from a non-linear regression of the pre-calculated LUT mentioned above. This three parameter function is adopted for the MSG-MPEF, because it has been shown to be superior over the performance of the other two models.

Chapter 3

Coefficients for Meteosat 8 (MSG-FM-1) and 9 (MSG-FM-2)

LUT's were generated for all the eight infrared channels of the SEVIRI instruments on Meteosat 8 (Meteosat Second Generation Flight Model 1, MSG-FM-1) and Meteosat 9 (MSG-FM-2) for the brightness temperature domain between 150 and 350 K with increments of 0.1 K. These LUT's were then used to derive the parameters of the non-linear regression model (eq. 2.4). The regression coefficients are listed in tables 7.2 and 7.3 for the Meteosat-8 and Meteosat-9 respectively.

The goodness of the derivation of the parameters are presented as a series of figures for each of the channels on both Meteosat-8 and -9. Figures 8.1 - 8.8 show a series of three panel figures. The top panel shows the variation of the brightness temperature as a function of effective radiances as provided by the non-linear regression model, with the parameters settings as presented in this panel. Also shown in this figure are selected entries from the pre-calculated look-up table indicated by the red symbols. The lower two panels represent the residuals between the LUT and the EBBT calculated with the three parametric non-linear regression model (2.4), with the parameters in tables 7.2 and 7.3 for the SEVIRI channels on Meteosat-8 (MSG-FM-1) and Meteosat-9 (MSG-FM-2) respectively. The bottom left panel shows the effective radiance residuals as function of effective radiances, while the right bottom panel shows the residuals as function of equivalent brightness temperatures. These panel shows that the brightness temperature residuals are a smooth function of radiance, and a root mean square difference of the order of 0.01 K or less is found, indicating the goodness of the approximation.

Chapter 4

Coefficients for MSG-FM-3 and -4.

Since the beginning of this project there has been several changes in relation to the conversion of effective radiances to brightness temperature.

In 2007/2008 EUMETSAT ran a study with the SEVIRI manufacturer to reprocess all SEVIRI ground characterization data in order to obtain a fully consistent set of instrument characterization in terms of effective radiance. One justification was to remove existing inconsistencies in the communication to the users.

The study results were compiled into an IMPF software and database re-design. Among other things this compilation contains spacecraft specific tables to relate temperatures to radiances as documented [RD.1] Since 2008, EUMETSAT answering to user enquiries in that respect has been with reference to the published tables. In line with this, the three parameter for the non-linear regression function for MSG-FM-3 and FM-4 have been generated to reproduce this table as accurately as possible.

The second important modification is that an alternative method to derive the non-linear regression parameters was implemented. The availability of the scripting language python allowed for a portable implementation of a non-linear regression method relatively simply. Although the intrinsic non-linear fitting routines will allow an accurate determination of the three parameters, the routines adopted here are taken from a collection of Python modules and applications developed by the computer group of the Kapteyn Astronomical Institute, University of Groningen, The Netherlands ([RD.2]) as this package provided some additional diagnostic tools.

The results for MSG-FM-3 and MSG-FM-4 are listed in tables 7.4 and 7.5. The goodness of the fits is shown in a similar way as discussed in section 3.

Chapter 5

Summary

The equivalent brightness temperature of an satellite observation, is defined as the temperature of a black body which emits the same amount of radiation as observed. Thus the brightness temperature follows from,

$$\bar{\mathcal{L}} = \int_{\Delta\nu} r_\nu L_\nu(p_t, \mu) d\nu / \int r_\nu d\nu. \tag{5.1}$$

with $\bar{\mathcal{L}}$ the observed radiances (in $mWm^{-2}sr^{-1}\left(cm^{-1}\right)^{-1}$), B the Planck function, T_b the equivalent brightness temperature (in kelvin units), ν wavenumber (in cm-1), and r_ν the instrument spectral response.

In the MSG-MPEF the following simple relation between the SEVIRI radiances and the equivalent brightness temperature is adopted:

$$\bar{\mathcal{L}} \approx \mathcal{C}_1 \nu_c^3 / \left(\exp\left(\mathcal{C}_2 \nu_c / \left[\alpha T_b + \beta\right]\right) - 1\right), \tag{5.2}$$

with $\mathcal{C}_1 = 2hc^2$ and $\mathcal{C}_2 = hc/k$ radiation constants where c, h, and k are the speed of light, Planck, and Boltzmann constant respectively (Values for these constants are listed in Table 7.1). The inverse of equation 5.2 reads

$$T_b = \frac{\mathcal{C}_2 \nu_c}{\alpha \log\left[\mathcal{C}_1 \nu_c^3 / \bar{\mathcal{R}} + 1\right]} - \frac{\beta}{\alpha}, \tag{5.3}$$

The regression coefficients ν_c, α and β are found from a non-linear regression of the pre-calculated lookup table, generated using equation 5.1, for the different SEVIRI channels. For Meteosat-8 and -9 this look-up table was generated as part of this process to determine the three parameters, wereas for MSG-FM-3 and FM-4 the lookup tables prepared by the IMPF were adopted.

Results of the non-linear regression are shown in tables 7.2 - 7.3 for Meteosat-8 and -9 respectively and in tables 7.4 - 7.5 for MSG-Flight model 3 and 4 respectively.

The goodness of the fit to the lookup tables is shown in figures 8.17 – 8.24 and figures 8.25 – 8.32 for MSG-FM3 and MSG-FM4 respectively.

Chapter 6

Reference Documents

[RD.1] Effective Radiances and Brightness Temperature Relation Tables for Meteosat Second Generation. EUM/OPS-MSG/TEN/08/0024, Issue v2. Available through http://www.eumetsat.int.
[RD.2] http://www.astro.rug.nl/software/kapteyn/index.html.
[RD.3] The 2010 CODATA from the NIST reference on Constants, Units and Uncertainty, from NIST Physical Measurement Laboratory http://www.nist.gov/cuu/index.html.

Chapter 7

Tables

7.1 General

Table 7.1: *Values for constants at time of writing [RD.3].*

Constant	Value
Speed of light in vacuum	299792458 ms^{-1}
Planck	6.62606957 10^{-34} Js
Bolzmann	1.3806488 10^{-23} JK^{-1}

7.2 Parameter tables

7.2.1 Table for Meteosat-8 (MSG FM-1)

Table 7.2: *Values for the regression parameters ν_c, α and β of the three parameter model evaluated using the non-linear regression analysis. The input LUT of radiances and brightness temperatures was calculated for brightness temperatures between 150 and 350 K with steps of 0.1 K. The values are valid for SEVIRI on Meteosat 8 (MSG Flight Model 1).*

Channel No.	Channel ID	ν_c[a]	α	β[b]
4	IR 3.9	2567.330	0.9956	3.410
5	WV 6.2	1598.103	0.9962	2.218
6	WV 7.3	1362.081	0.9991	0.478
7	IR 8.7	1149.069	0.9996	0.179
8	IR 9.7	1034.343	0.9999	0.060
9	IR 10.8	930.647	0.9983	0.625
10	IR 12.0	839.660	0.9988	0.397
11	IR 13.4	752.387	0.9981	0.578

[a] Units: cm^{-1}.
[b] Units: K.

7.2.2 Table for Meteosat-9 (MSG FM-2)

Table 7.3: *Values for the regression parameters ν_c, α and β of the three parameter model evaluated using the non-linear regression analysis. The input LUT of radiances and brightness temperatures was calculated for brightness temperatures between 150 and 350 K with steps of 0.1 K. The values are valid for SEVIRI on Meteosat 9 (MSG Flight Model 2).*

Channel No.	Channel ID	ν_c[a]	α	β[b]
4	IR 3.9	2568.832	0.9954	3.438
5	WV 6.2	1600.548	0.9963	2.185
6	WV 7.3	1360.330	0.9991	0.470
7	IR 8.7	1148.620	0.9996	0.179
8	IR 9.7	1035.289	0.9999	0.056
9	IR 10.8	931.700	0.9983	0.640
10	IR 12.0	836.445	0.9988	0.408
11	IR 13.4	751.792	0.9981	0.561

[a] Units: cm^{-1}.
[b] Units: K.

7.2.3 Table for MSG FM-3

Table 7.4: *Values for the regression parameters ν_c, α and β of the three parameter model evaluated using the kapteyn non-linear regression module (http://www.astro.rug.nl/software/kapteyn/index.html) for the different channels on MSG flight model 3. The input LUT of radiances and brightness temperatures were taken from the IMPF radiance and brightness temperatures.*

Channel No.	Channel ID	ν_c[a]	α	β[b]
4	IR 3.9	2547.771	0.9915	2.9002
5	WV 6.2	1595.621	0.9960	2.0337
6	WV 7.3	1360.377	0.9991	0.4340
7	IR 8.7	1148.130	0.9996	0.1714
8	IR 9.7	1034.715	0.9999	0.0527
9	IR 10.8	929.842	0.9983	0.6084
10	IR 12.0	838.659	0.9988	0.3882
11	IR 13.4	750.653	0.9982	0.5390

[a] Units: cm^{-1}.
[b] Units: K.

7.2.4 Table for MSG FM-4

Table 7.5: *Values for the regression parameters ν_c, α and β of the three parameter model evaluated using the kapteyn non-linear regression module ((http://www.astro.rug.nl/software/kapteyn/index.html)) for the different channels on MSG flight model 4. The input LUT of radiances and brightness temperatures were taken from the IMPF radiance and brightness temperatures.*

Channel No.	Channel ID	ν_c[a]	α	β[b]
4	IR 3.9	2555.280	0.9916	2.9438
5	WV 6.2	1596.080	0.9959	2.0780
6	WV 7.3	1361.748	0.9990	0.4929
7	IR 8.7	1147.433	0.9996	0.1731
8	IR 9.7	1034.851	0.9998	0.0597
9	IR 10.8	931.122	0.9983	0.6256
10	IR 12.0	839.113	0.9988	0.4002
11	IR 13.4	748.585	0.9981	0.5635

[a] Units: cm^{-1}.
[b] Units: K.

Chapter 8

Figures

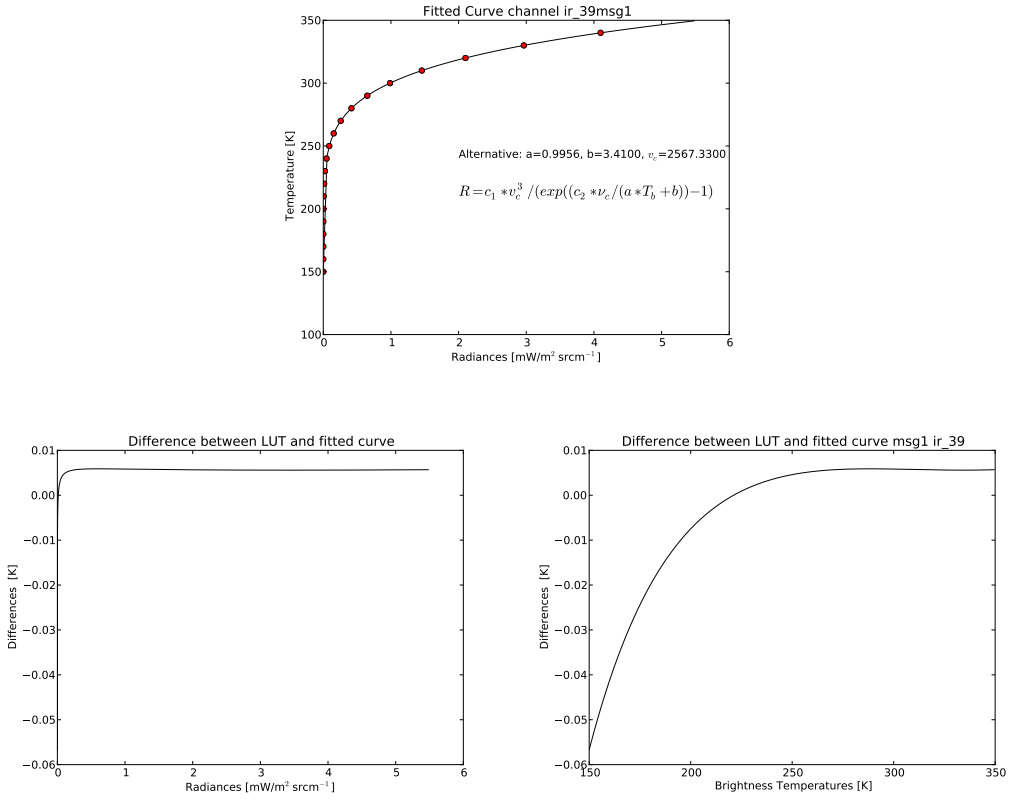

Figure 8.1: Result of the non-linear regression for ir 39 on Meteosat 8 (MSG-FM-1).

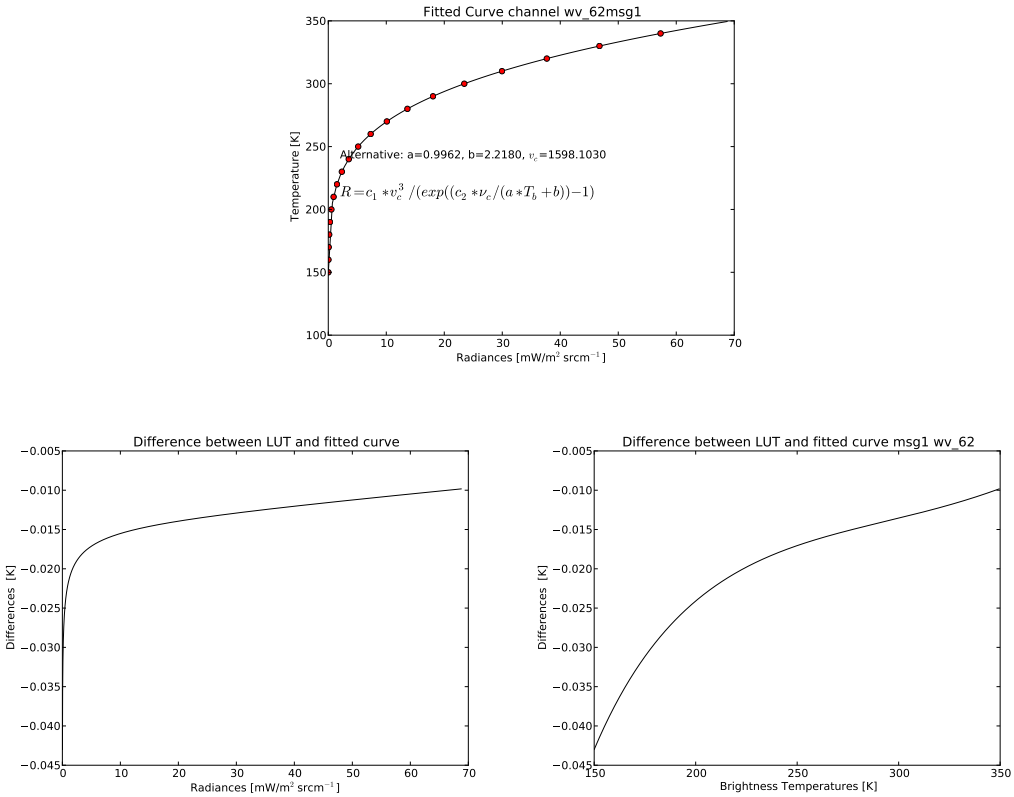

Figure 8.2: Result of the non-linear regression for wv 62 on Meteosat 8 (MSG-FM-1).

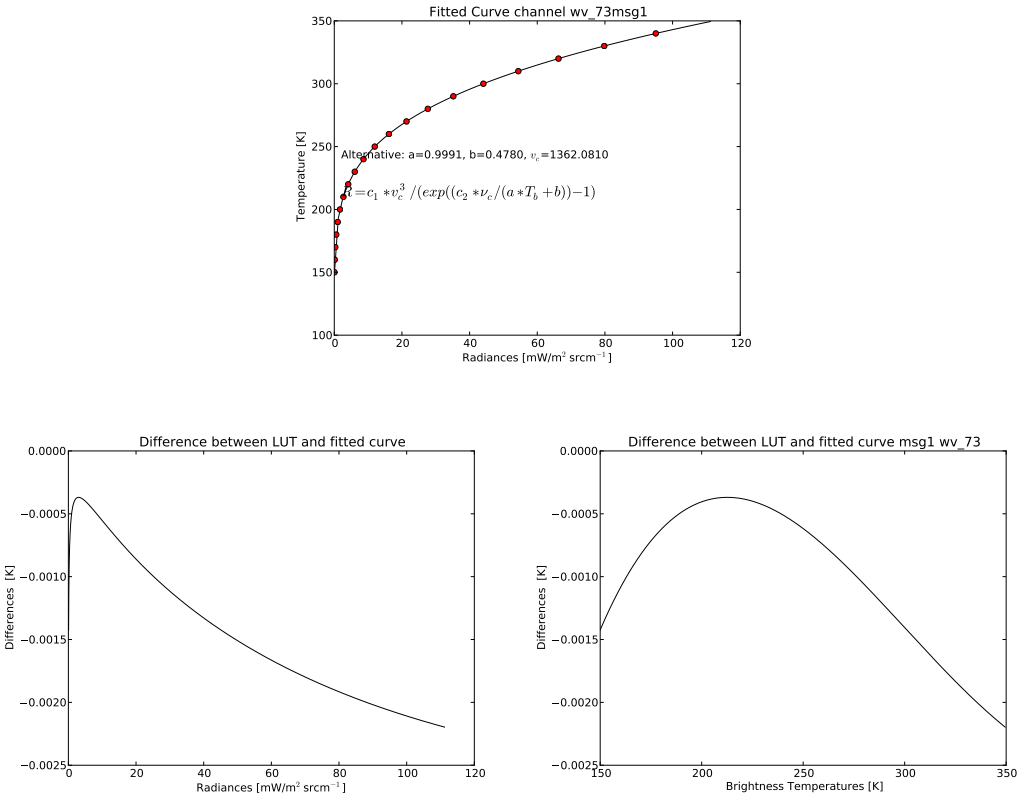

Figure 8.3: Result of the non-linear regression for wv 73 on Meteosat 8 (MSG-FM-1).

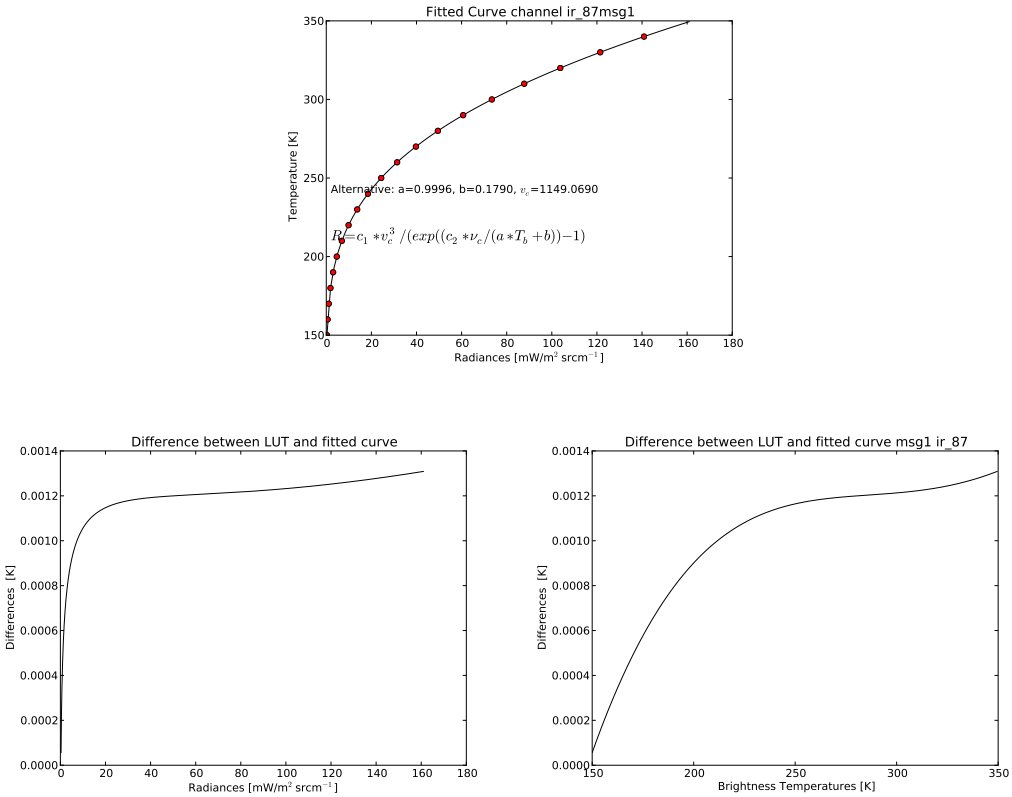

Figure 8.4: Result of the non-linear regression for ir 87 on Meteosat 8 (MSG-FM-1).

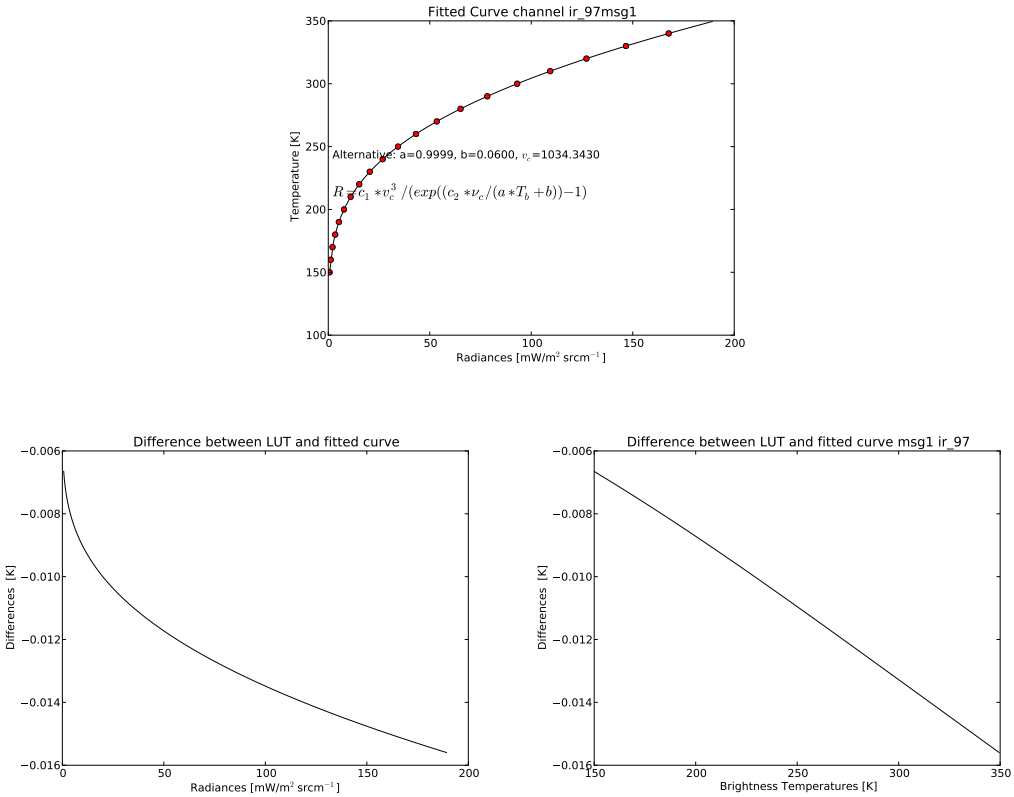

Figure 8.5: Result of the non-linear regression for ir 97 on Meteosat 8 (MSG-FM-1).

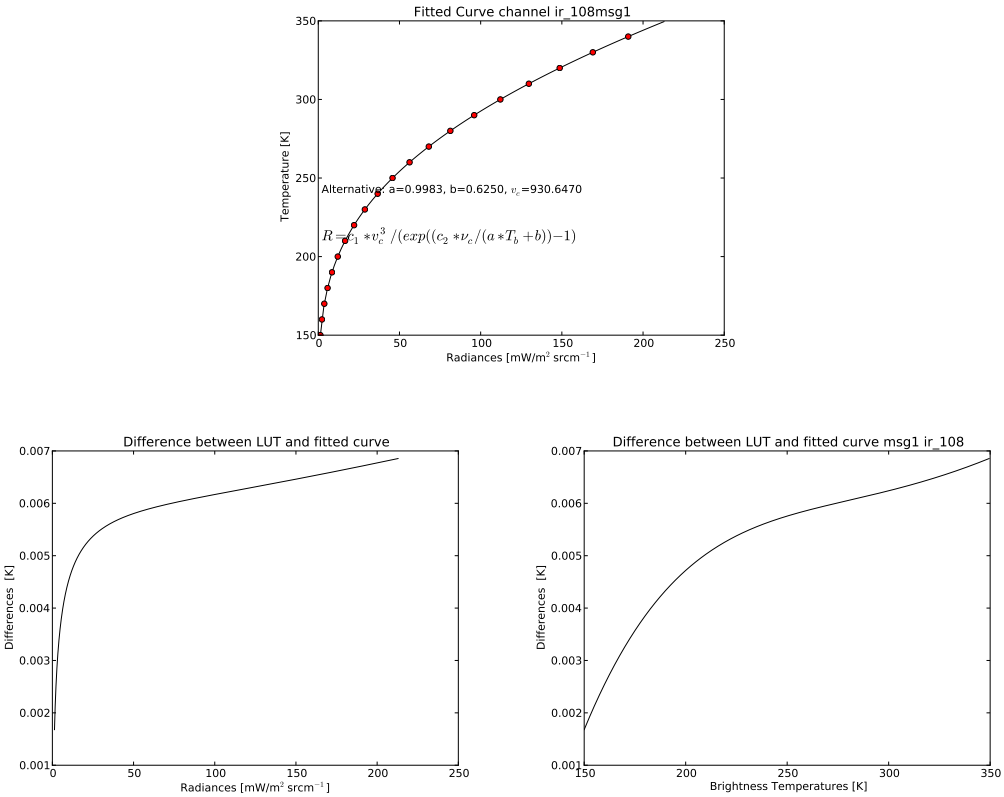

Figure 8.6: Result of the non-linear regression for ir 108 on Meteosat 8 (MSG-FM-1).

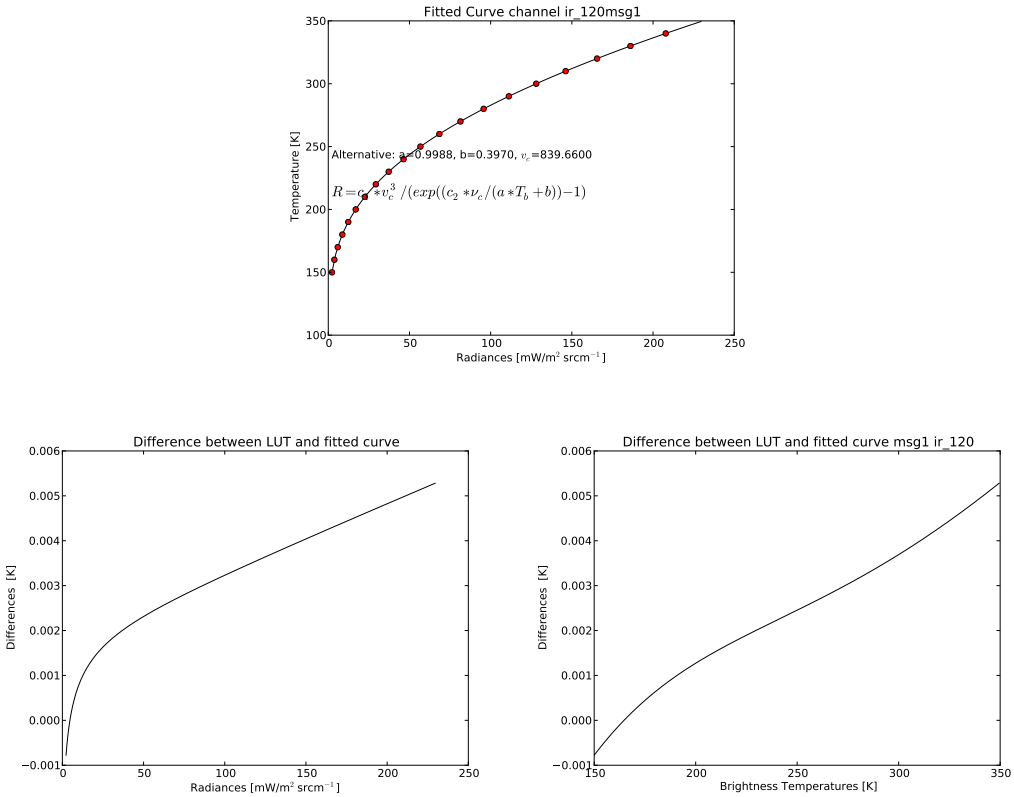

Figure 8.7: Result of the non-linear regression for ir 120 on Meteosat 8 (MSG-FM-1).

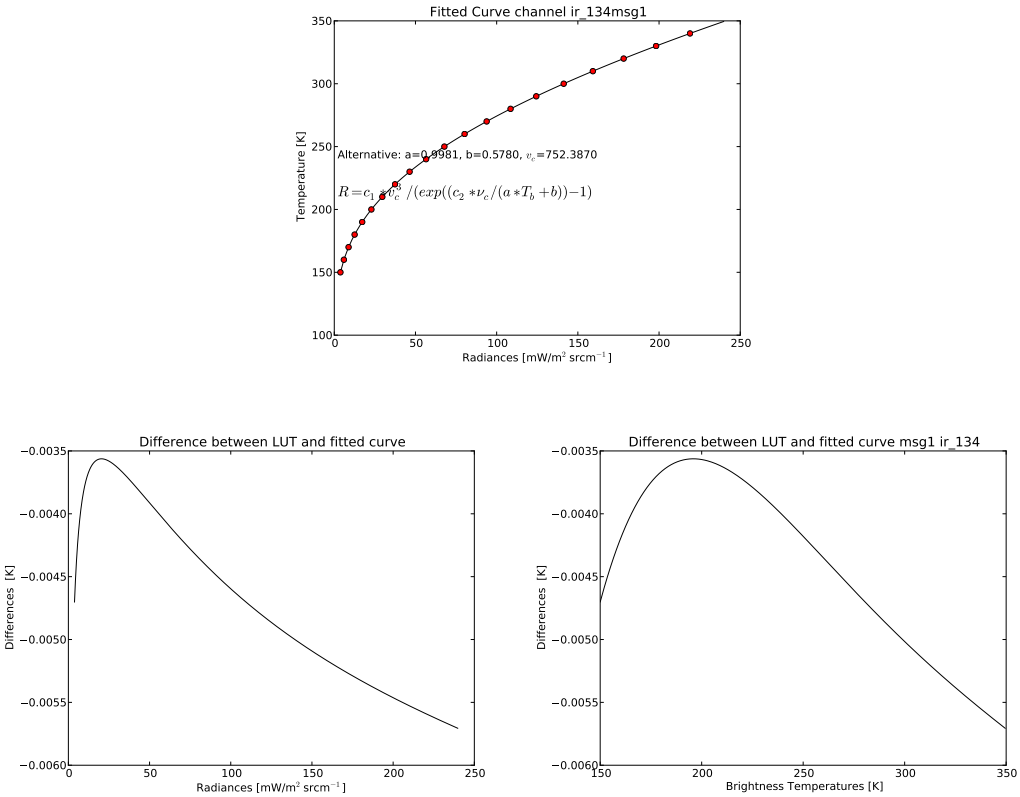

Figure 8.8: Result of the non-linear regression for ir 134 on Meteosat 8 (MSG-FM-1).

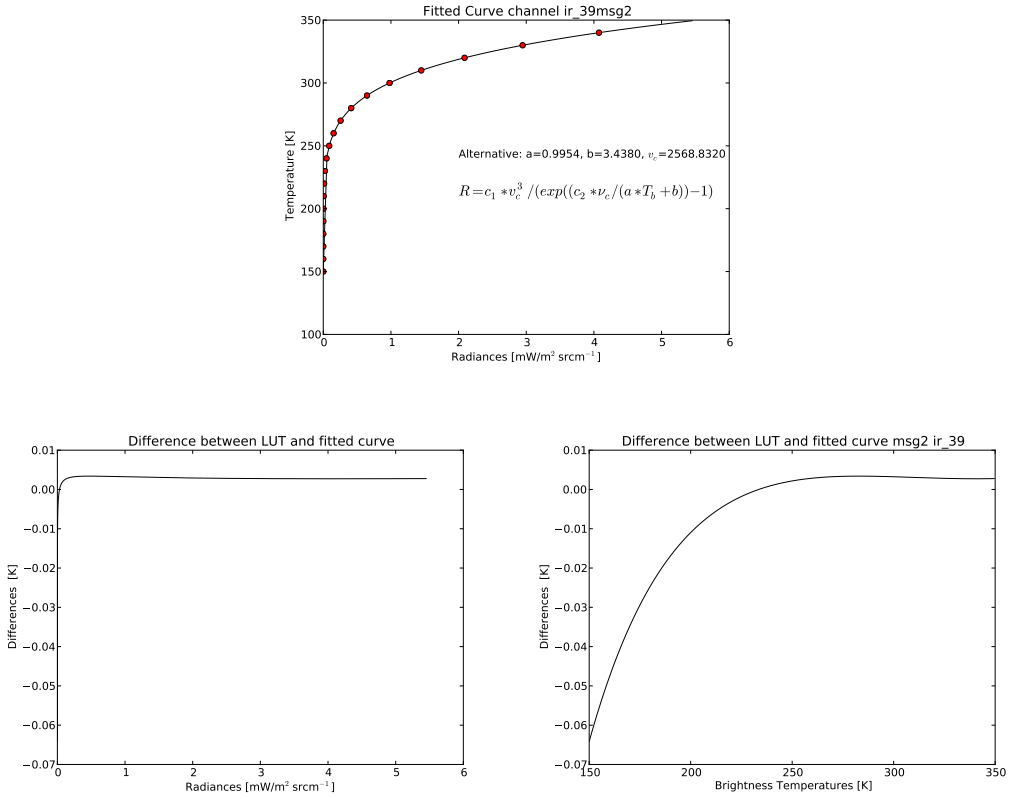

Figure 8.9: Result of the non-linear regression for ir 39 on Meteosat 9 (MSG-FM-2).

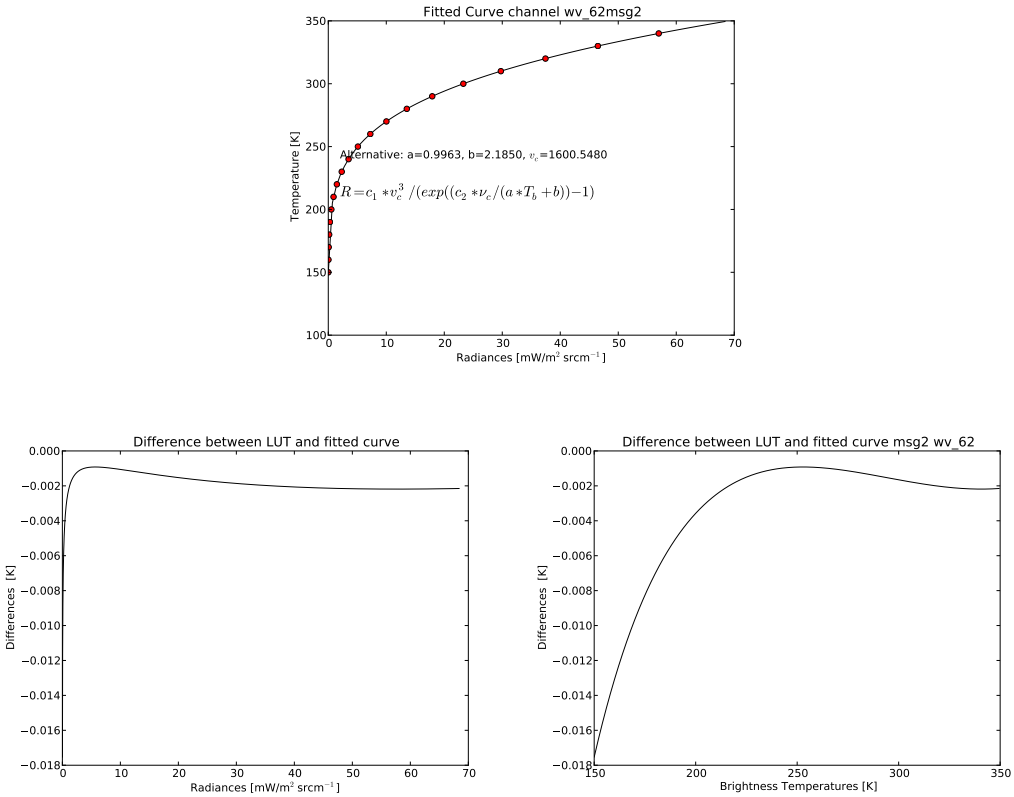

Figure 8.10: Result of the non-linear regression for wv 62 on Meteosat 9 (MSG-FM-2).

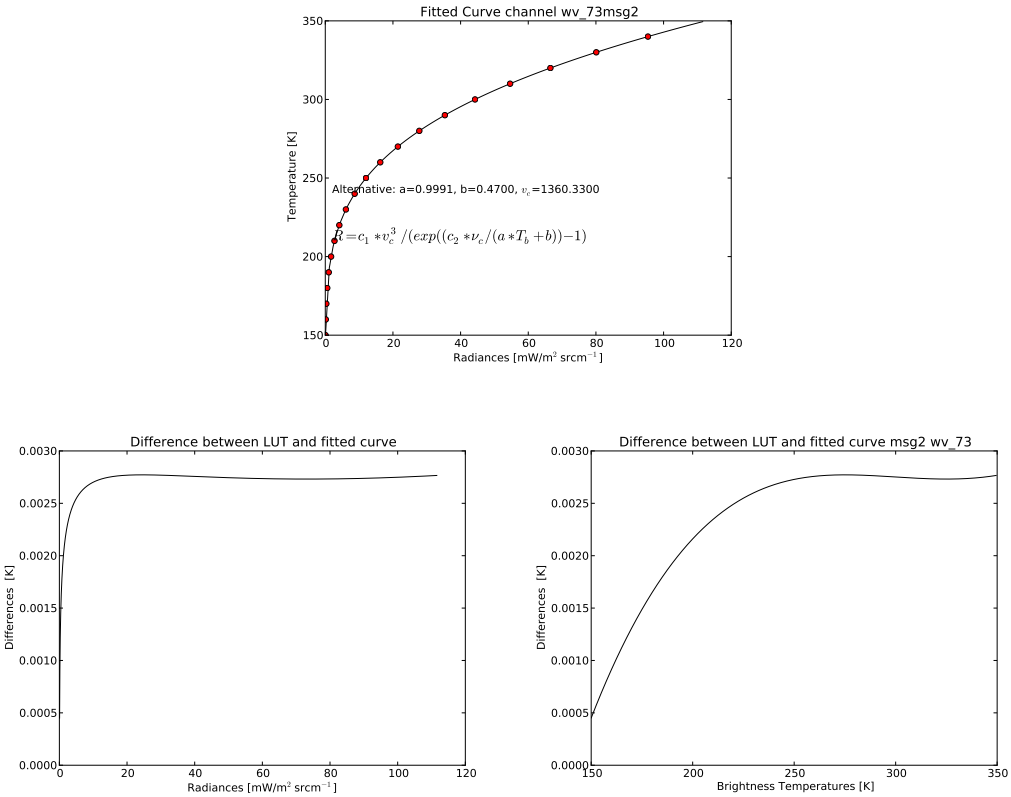

Figure 8.11: Result of the non-linear regression for wv 73 on Meteosat 9 (MSG-FM-2).

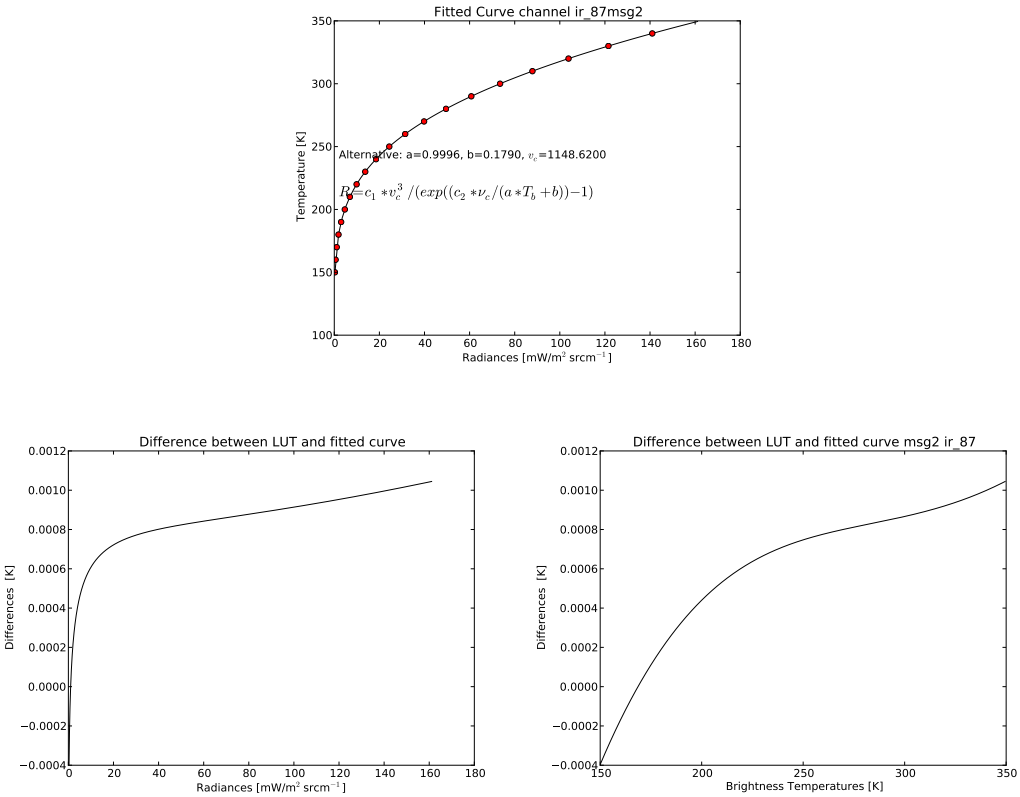

Figure 8.12: Result of the non-linear regression for ir 87 on Meteosat 9 (MSG-FM-2).

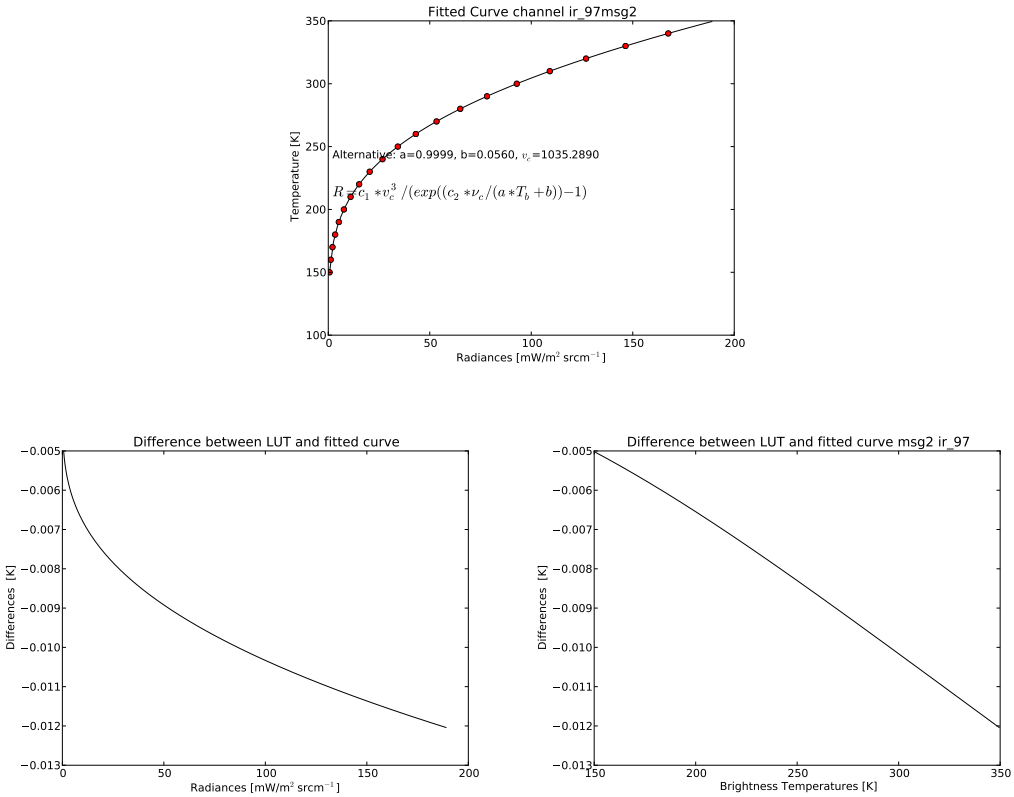

Figure 8.13: Result of the non-linear regression for ir 97 on Meteosat 9 (MSG-FM-2).

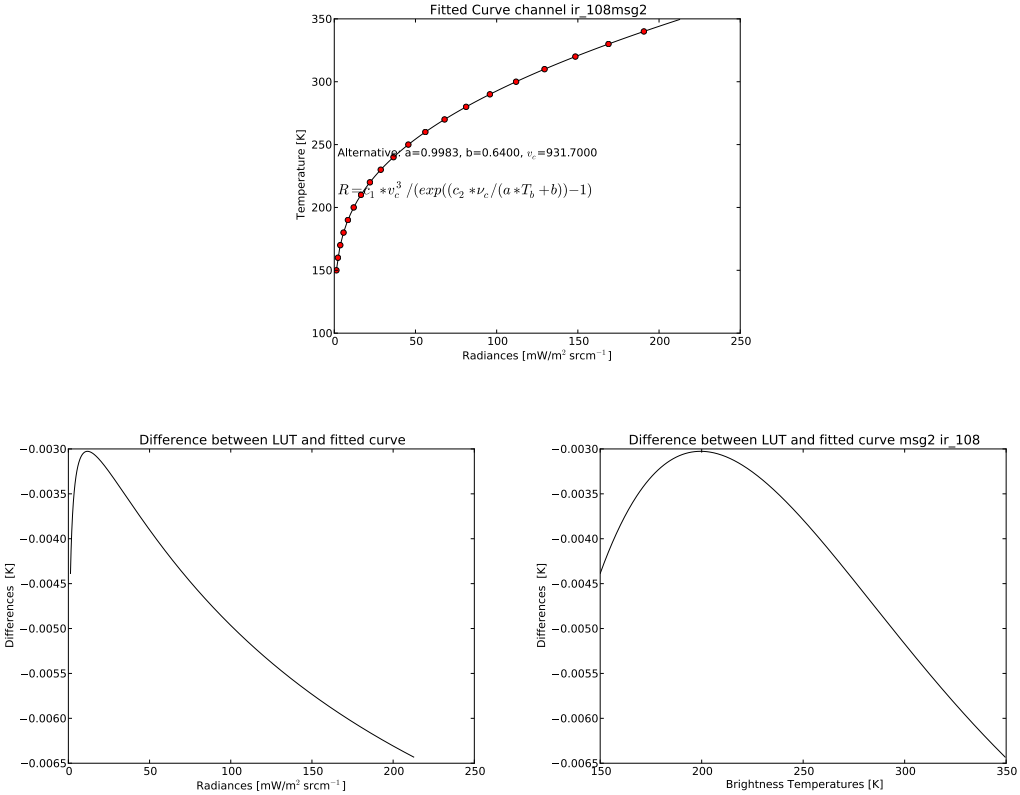

Figure 8.14: Result of the non-linear regression for ir 108 on Meteosat 9 (MSG-FM-2).

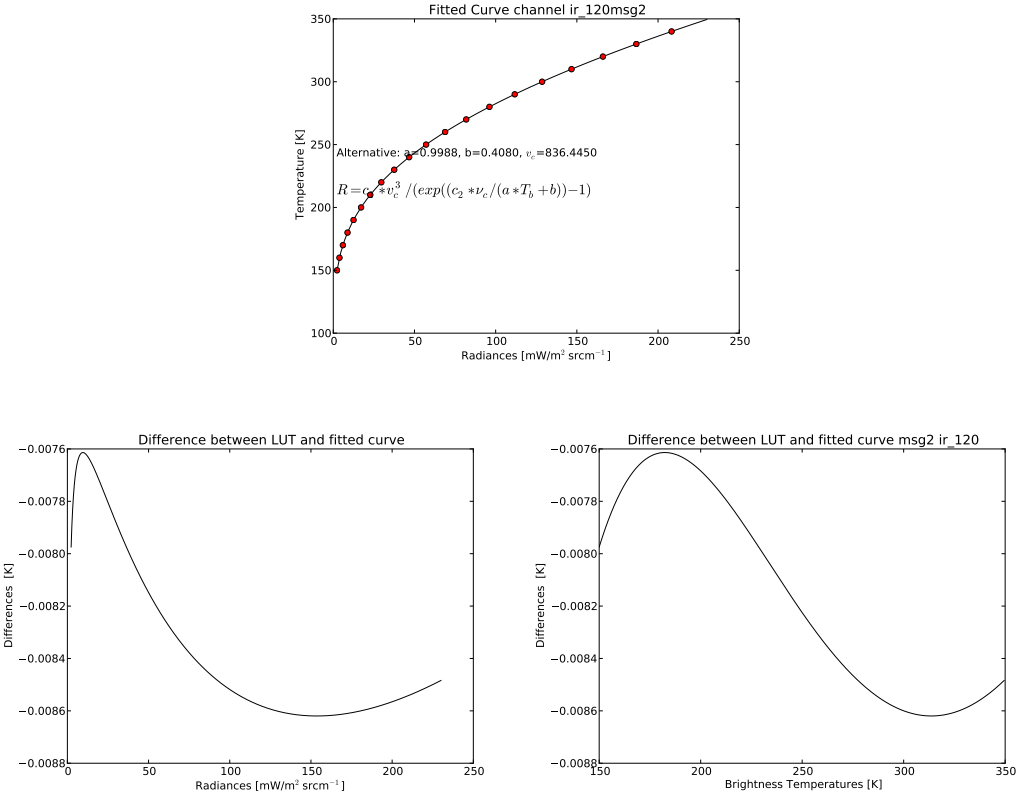

Figure 8.15: Result of the non-linear regression for ir 120 on Meteosat 9 (MSG-FM-2).

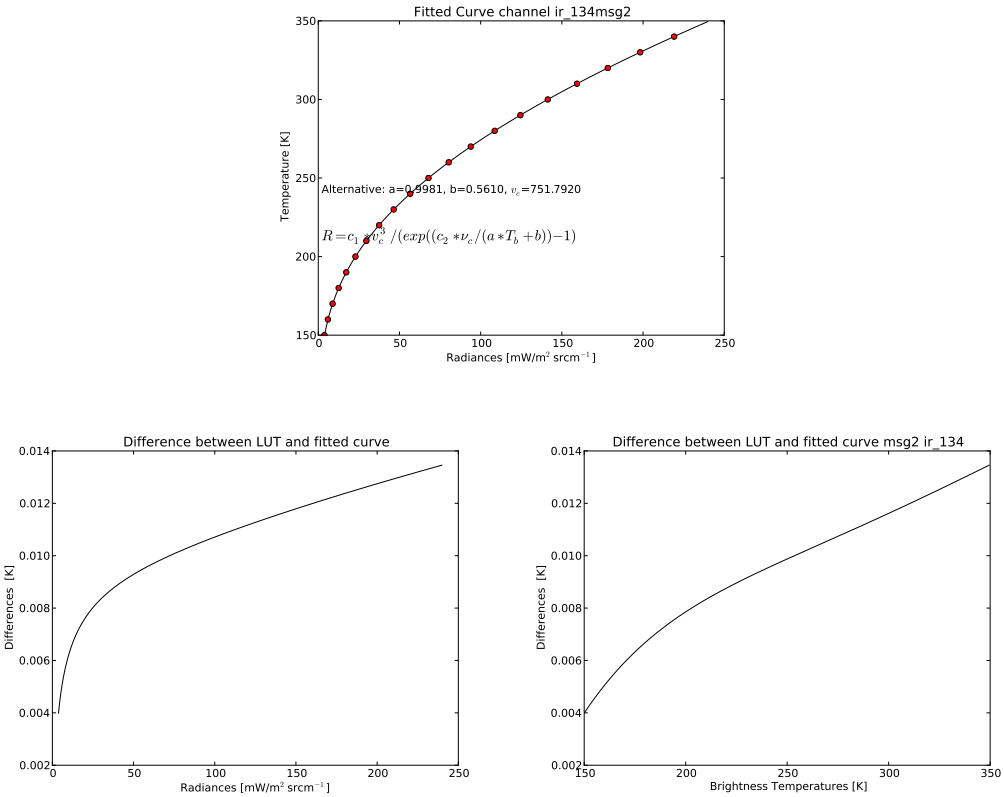

Figure 8.16: Result of the non-linear regression for ir 134 on Meteosat 9 (MSG-FM-2).

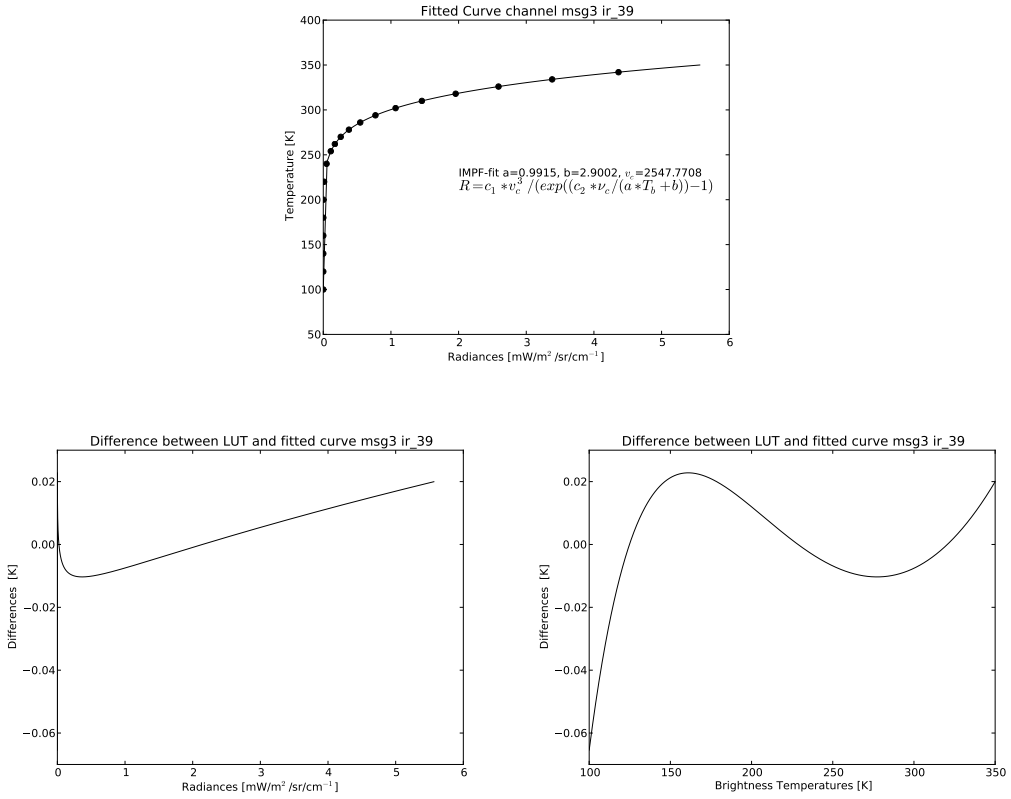

Figure 8.17: Result of the non-linear regression for ir 39 on MSG FM3.

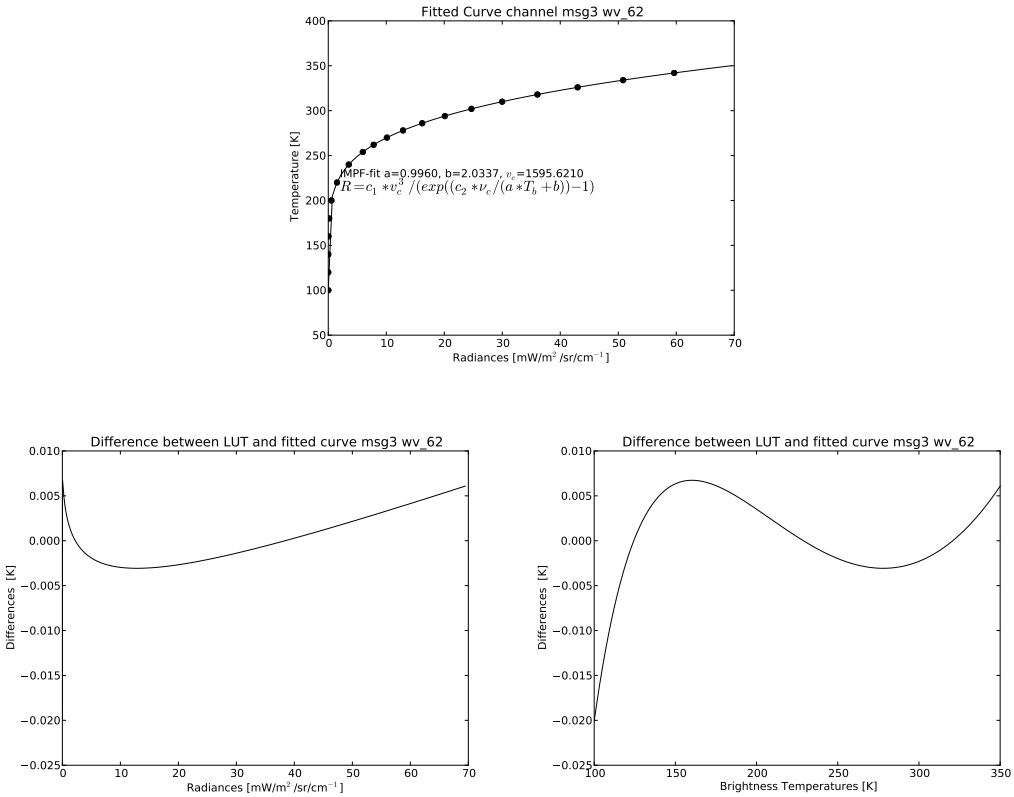

Figure 8.18: Result of the non-linear regression for wv 62 on MSG FM3.

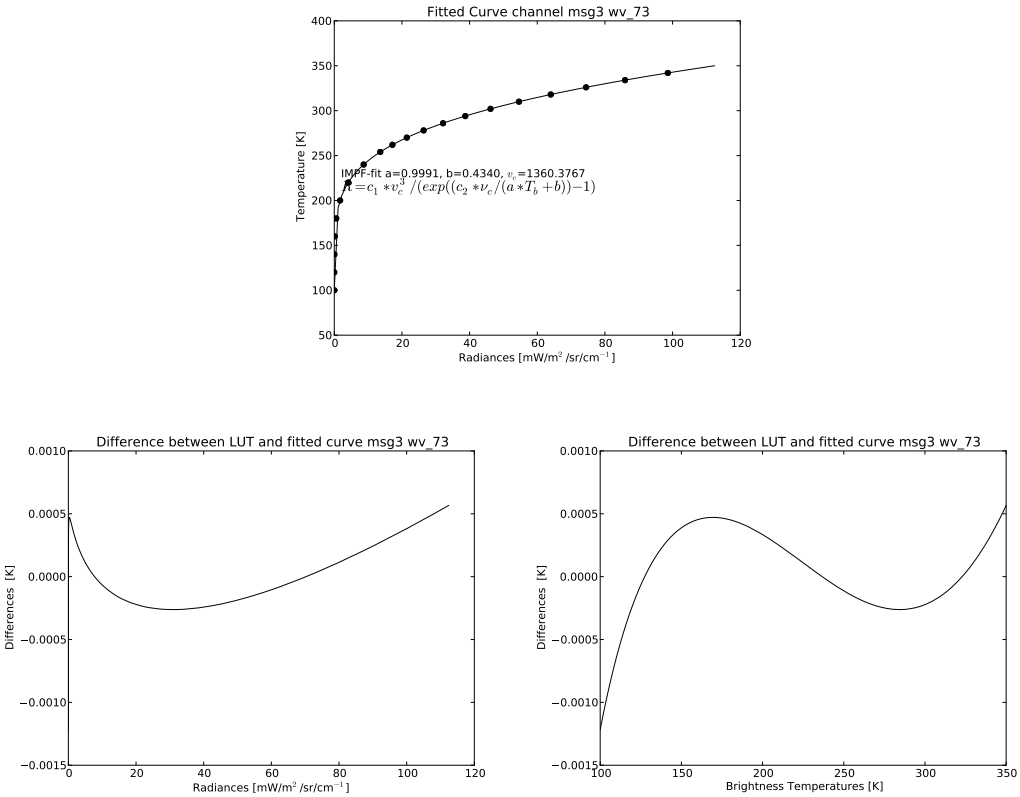

Figure 8.19: Result of the non-linear regression for wv 73 on MSG FM3.

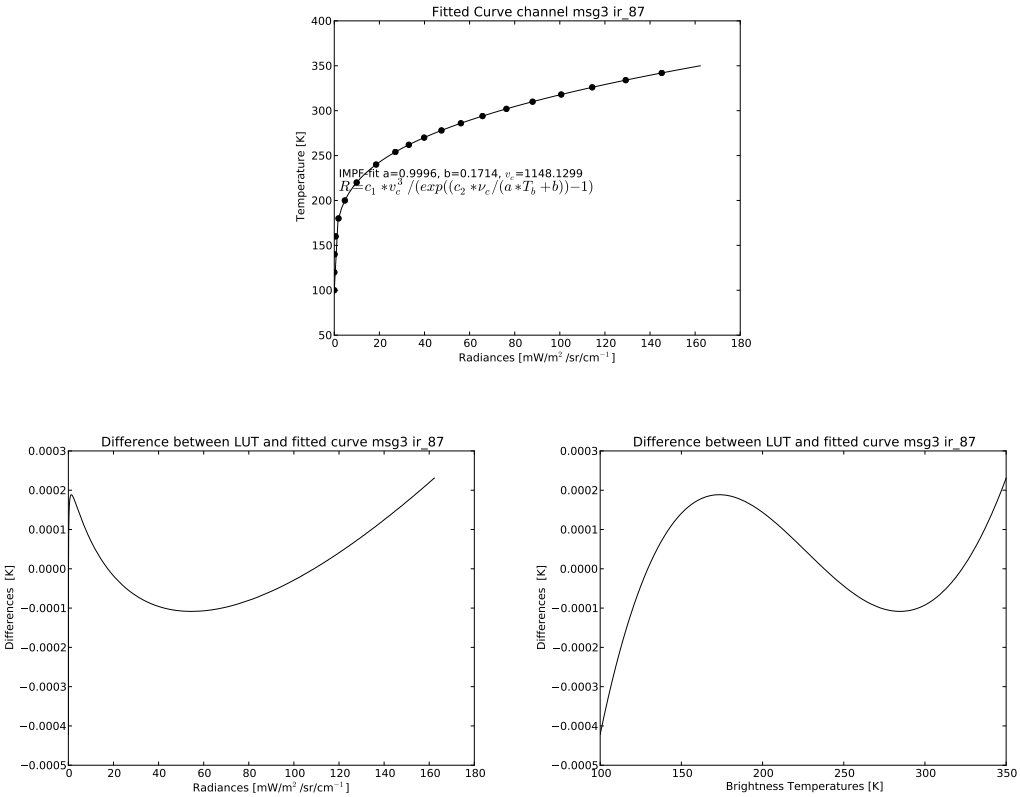

Figure 8.20: Result of the non-linear regression for ir 87 on MSG FM3.

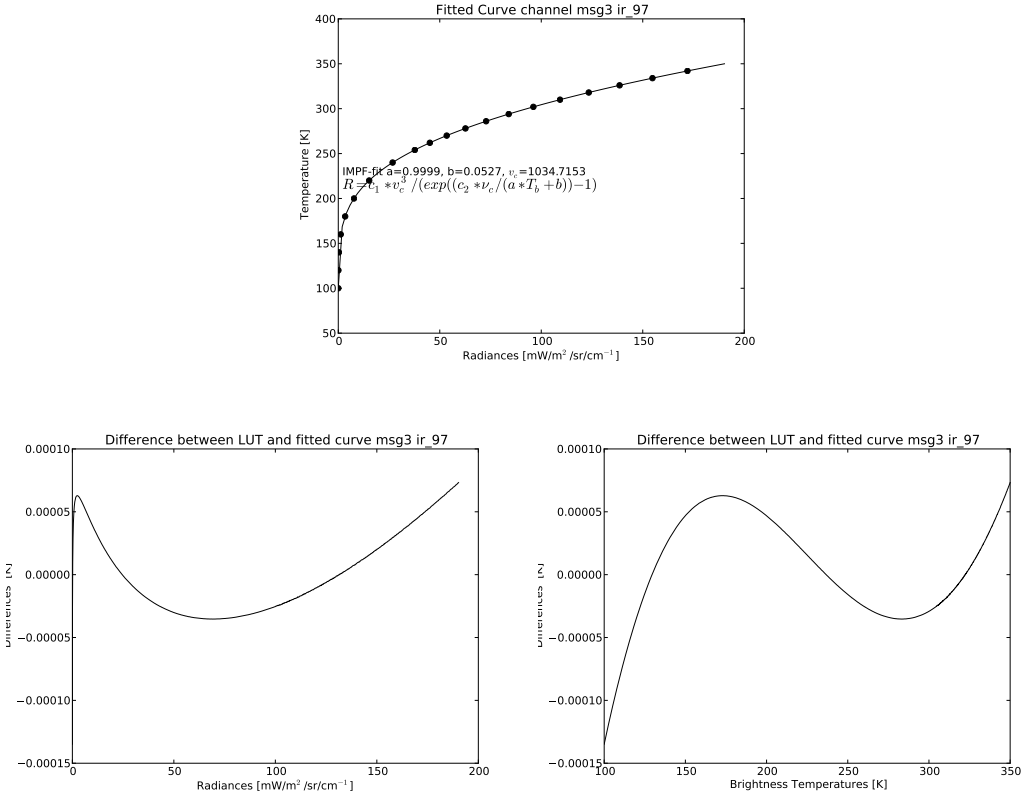

Figure 8.21: Result of the non-linear regression for ir 97 on MSG FM3.

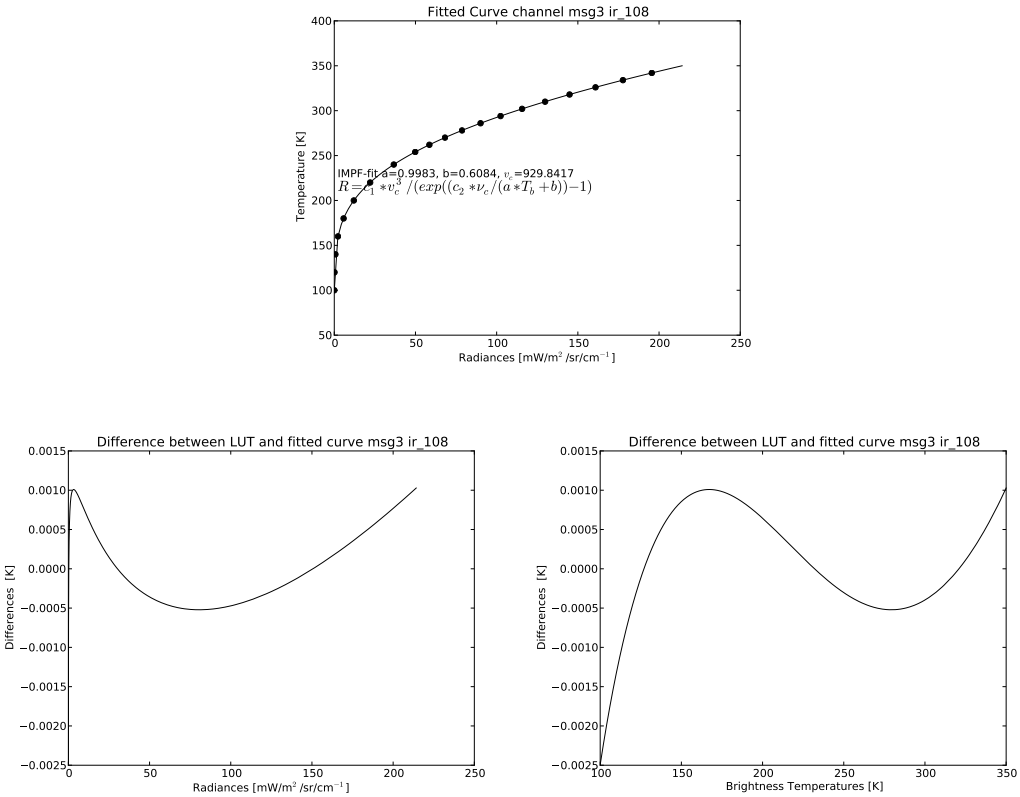

Figure 8.22: Result of the non-linear regression for ir 108 on MSG FM3.

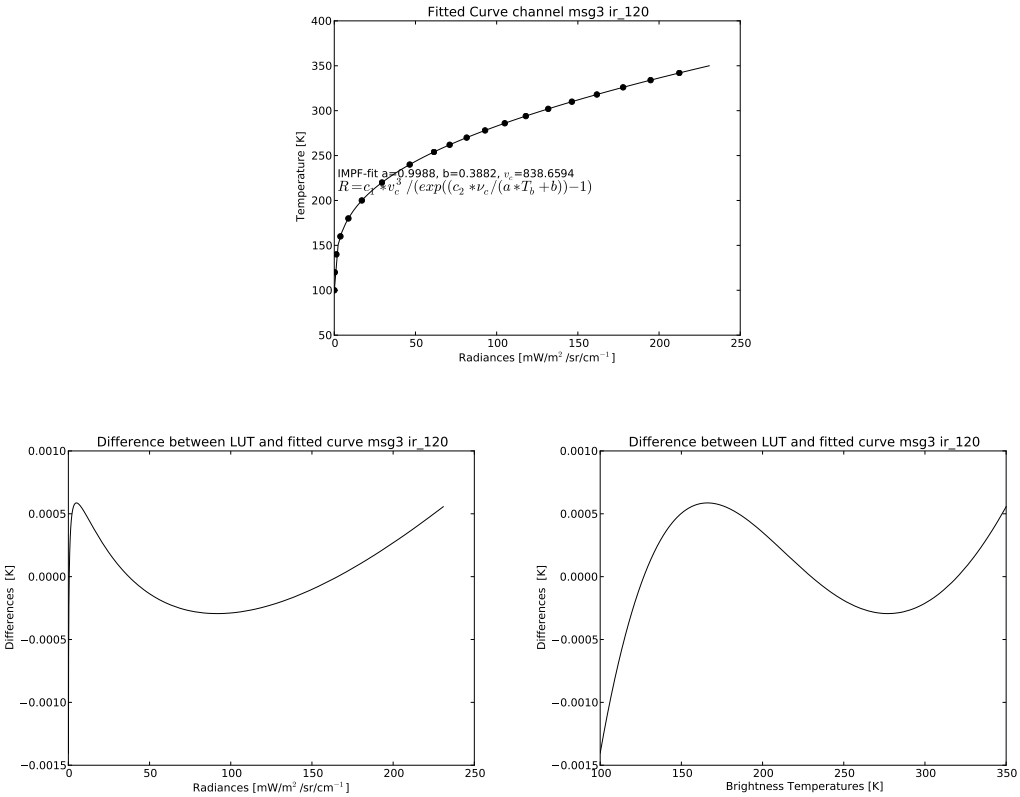

Figure 8.23: Result of the non-linear regression for ir 120 on MSG FM3.

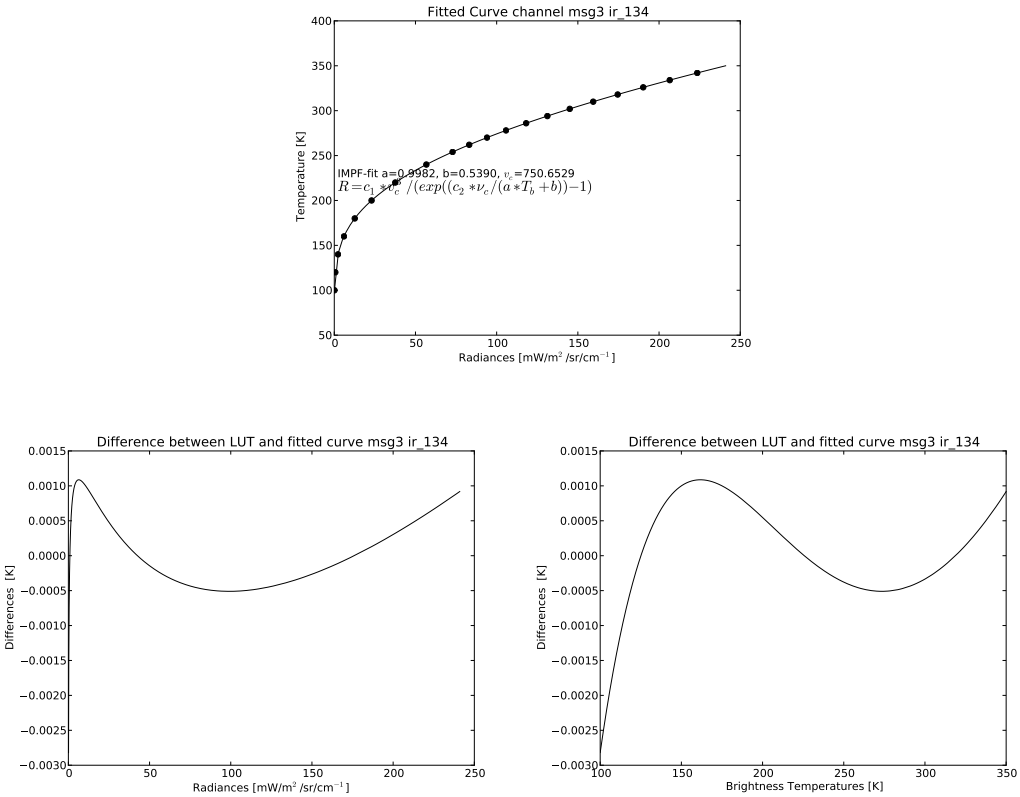

Figure 8.24: Result of the non-linear regression for ir 134 on MSG FM3.

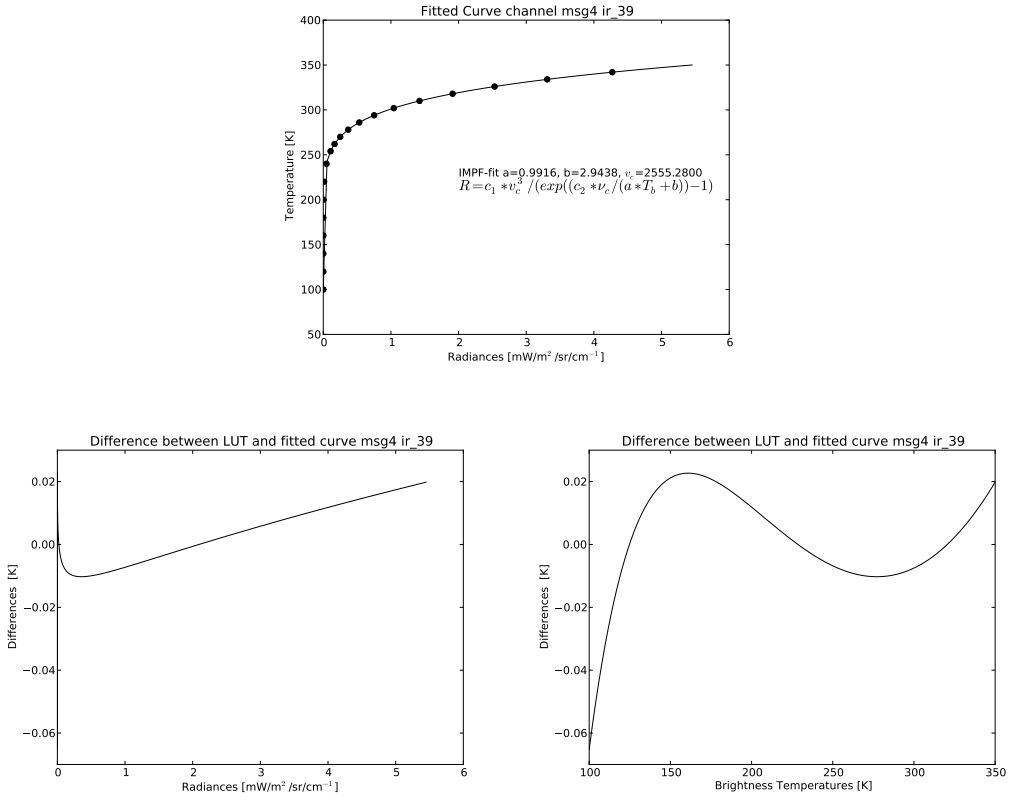

Figure 8.25: Result of the non-linear regression for ir 39 on MSG FM4.

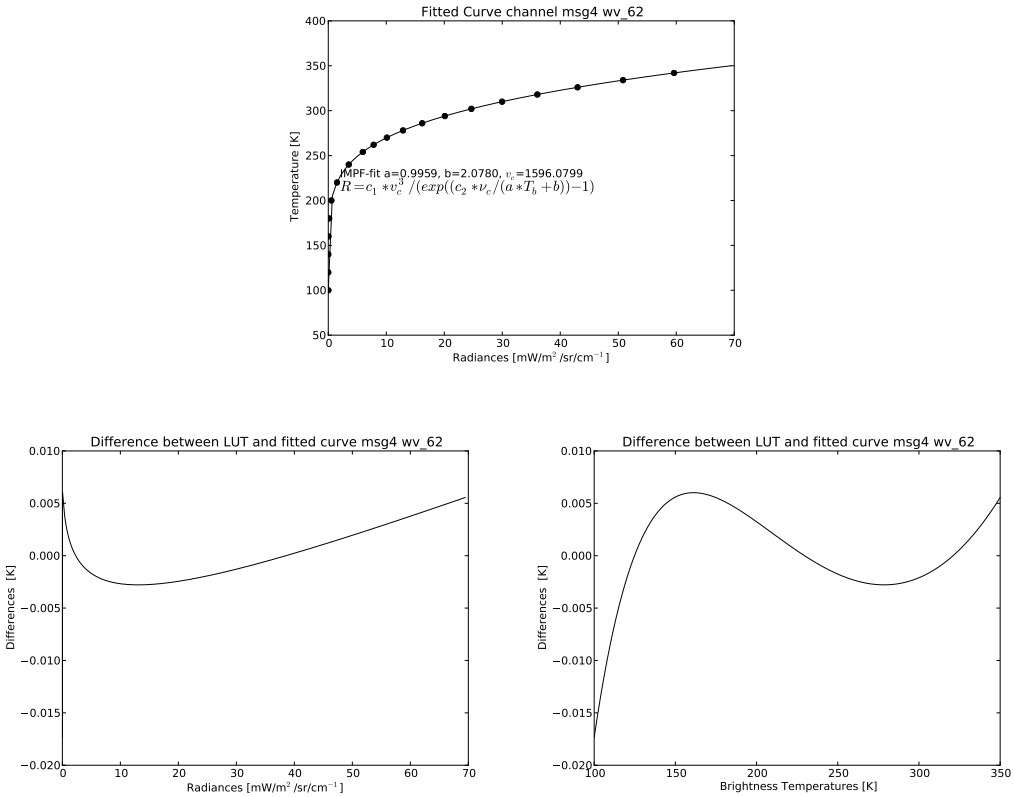

Figure 8.26: Result of the non-linear regression for wv 62 on MSG FM4.

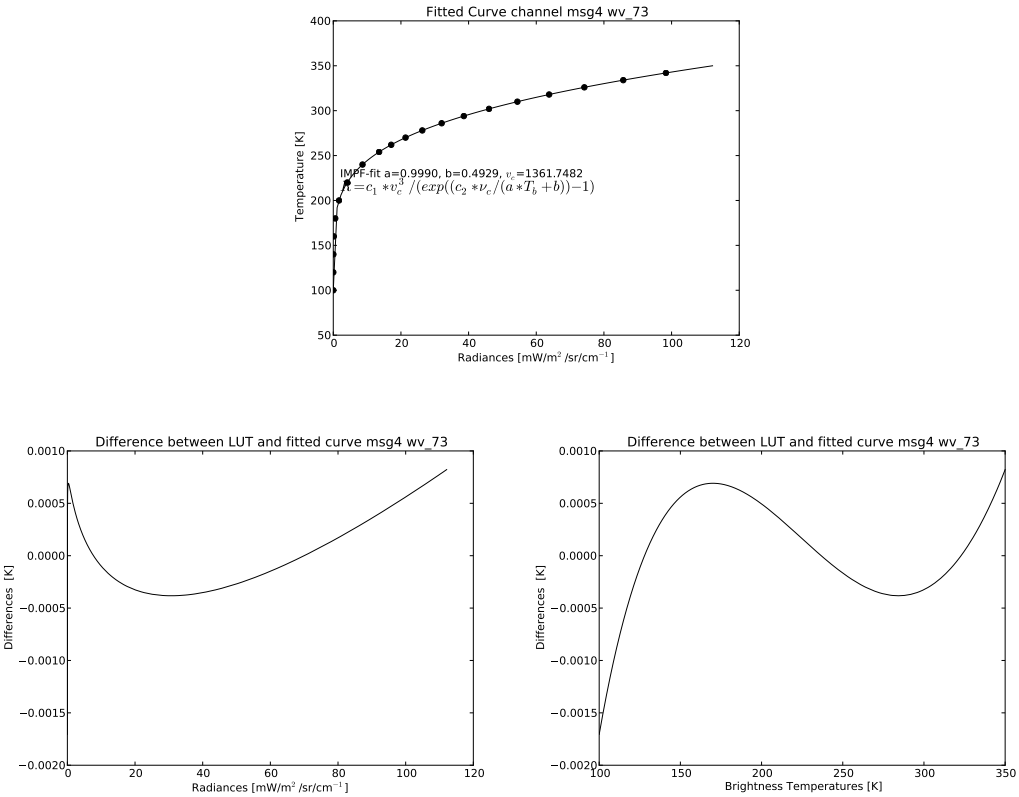

Figure 8.27: Result of the non-linear regression for wv 73 on MSG FM4.

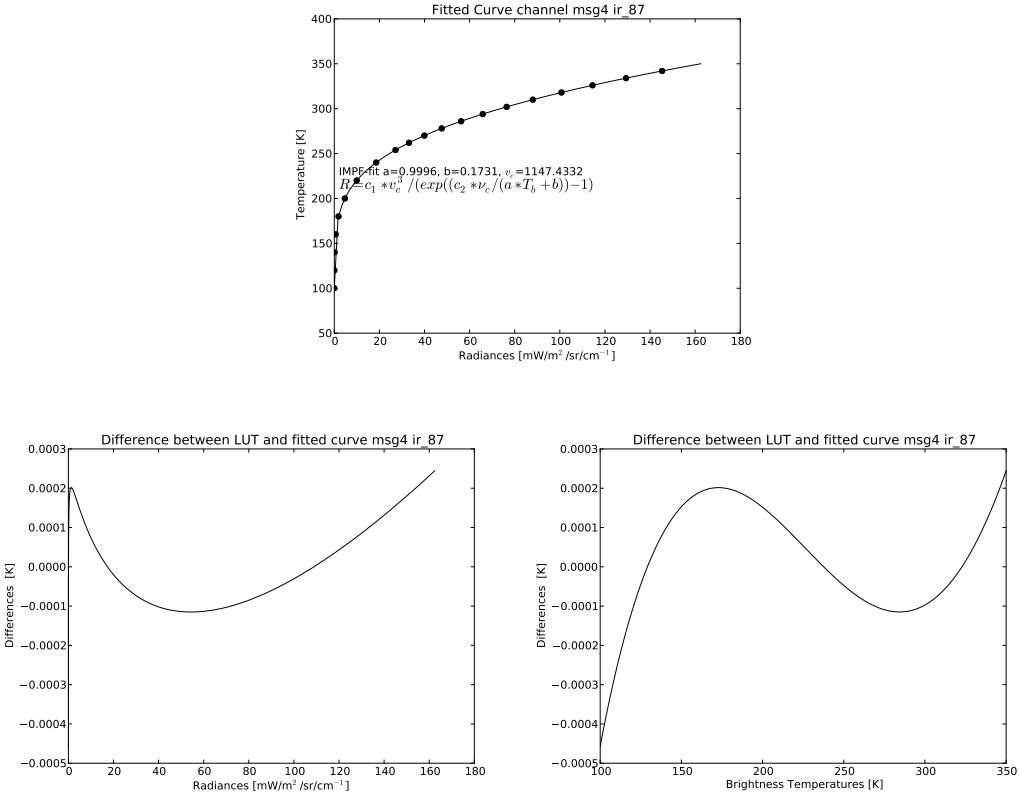

Figure 8.28: Result of the non-linear regression for ir 87 on MSG FM4.

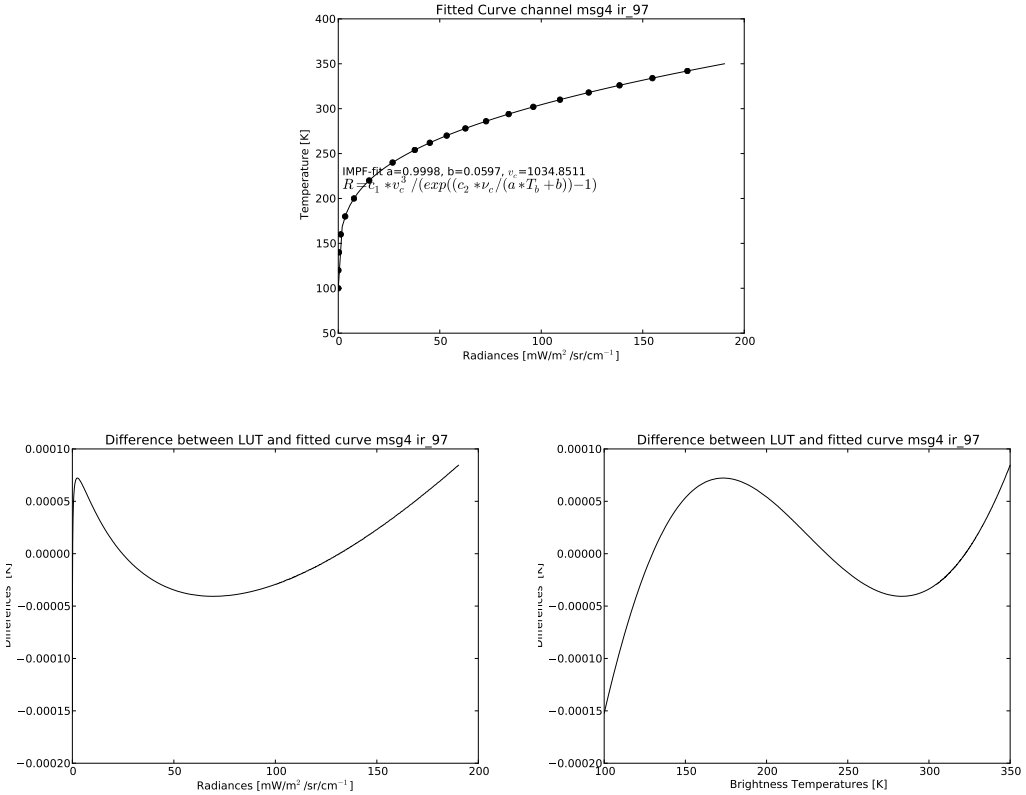

Figure 8.29: Result of the non-linear regression for ir 97 on MSG FM4.

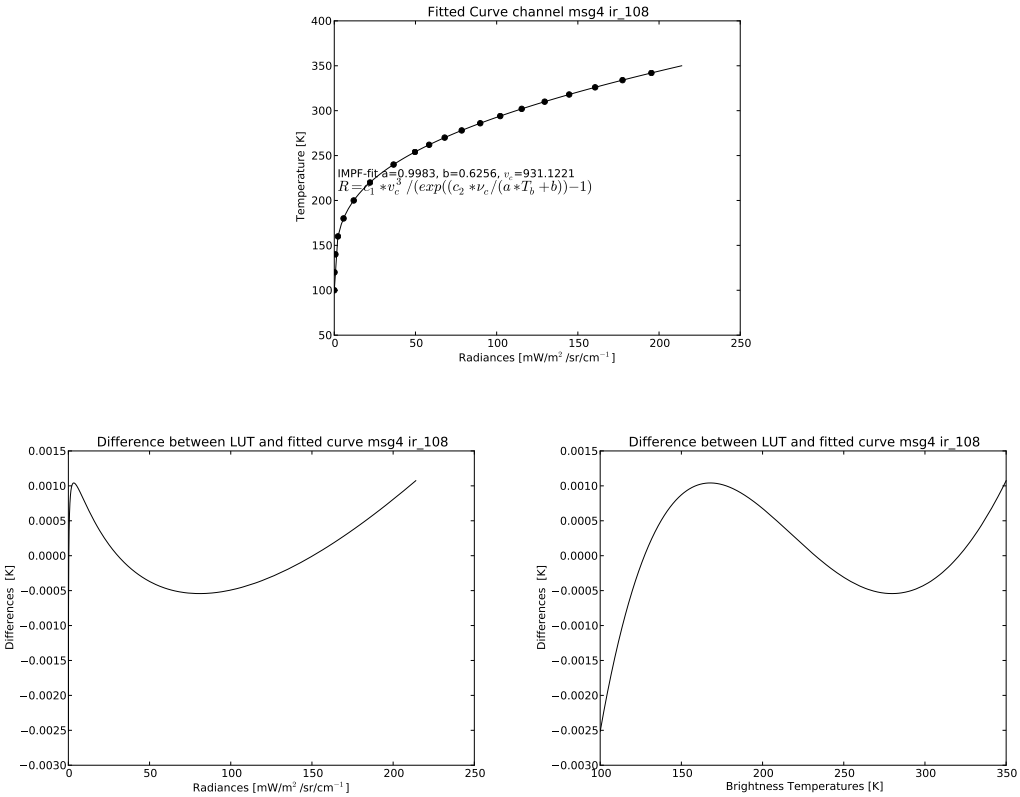

Figure 8.30: Result of the non-linear regression for ir 108 on MSG FM4.

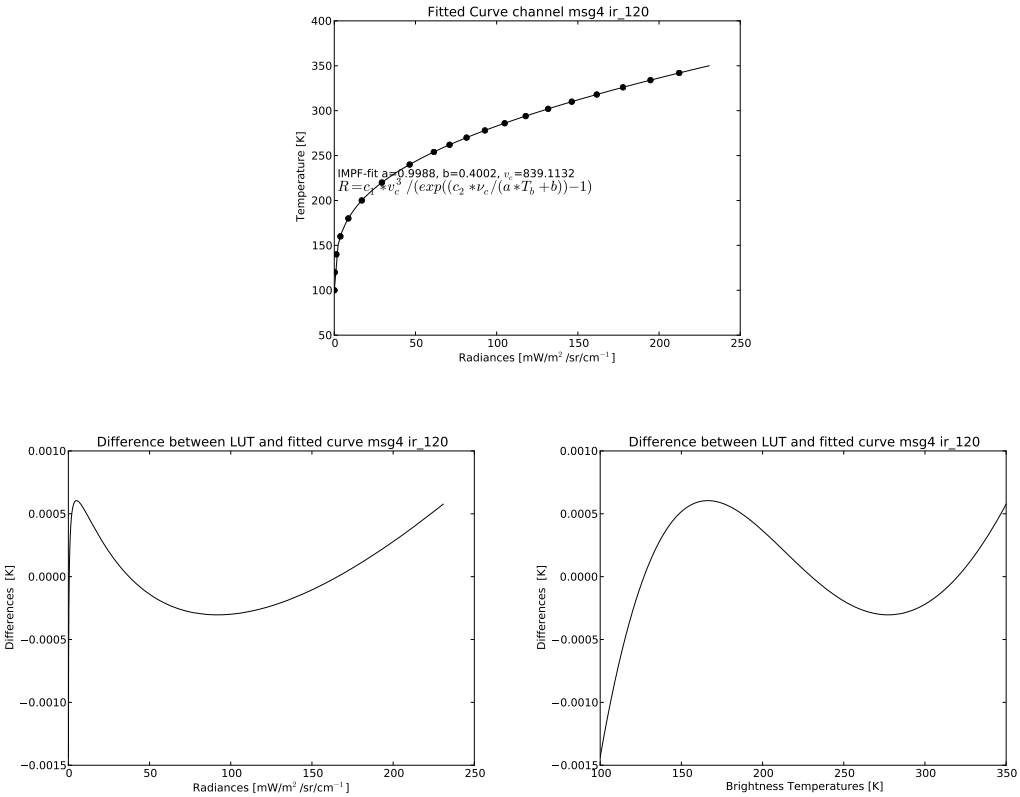

Figure 8.31: Result of the non-linear regression for ir 120 on MSG FM4.

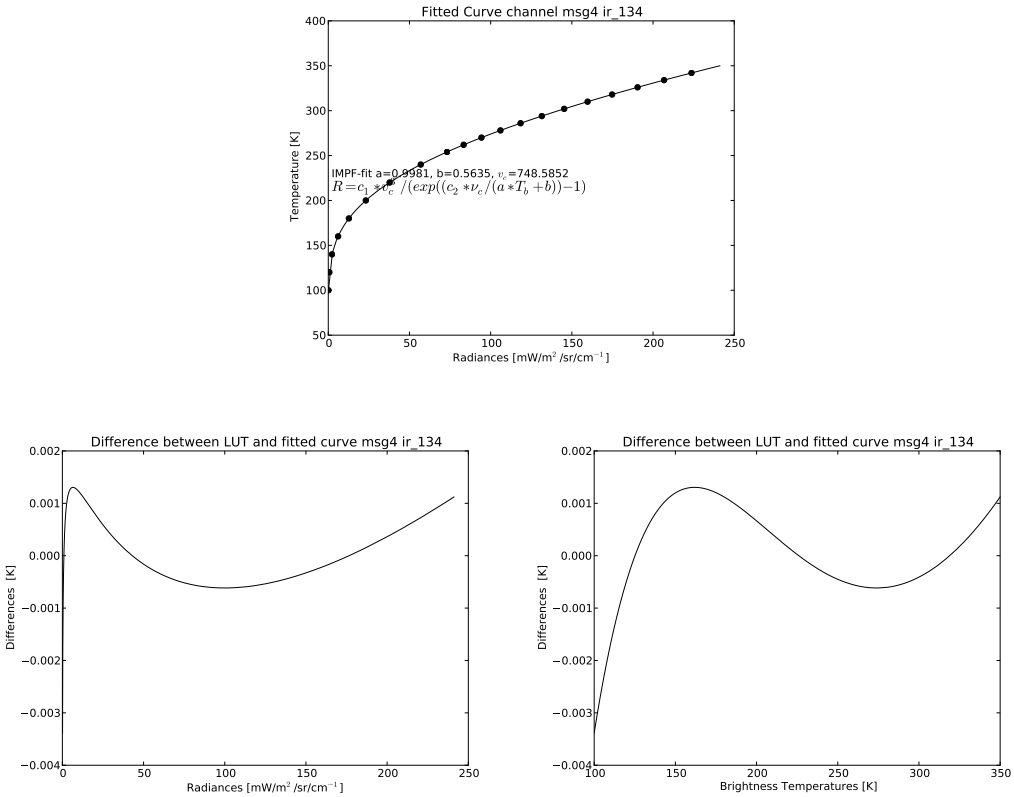

Figure 8.32: Result of the non-linear regression for ir 134 on MSG FM4.